Proceedings World Geothermal Congress 2020+1
Reykjavik, Iceland, April - October 2021

# Fitness for Service Assessment of Geothermal Steam Turbines

Stephen Rowbotham, Sean Norburn and Cole Davis

1965 57th Court North, Boulder, Colorado, 80301, USA

S.Rowbotham@questintegrity.com

**Keywords:** Fitness for Service, Finite Element Analysis, Modelling, Geothermal Steam, Flash Cavitation/Wire Drawing, Failure Assessment Diagram

## ABSTRACT

Geothermal tuebines operate in severe operating conditions with aggressive steam and carryover of particulates into the steam path. Operational campaigns of 4 years or more are typically followed by inspection and condition assessment to identify any degradation that may require decision making, for repair or component replacement, to return the asset to service as quickly as possible. The paper will look at the steps and processes involved in completing a fitness for service assessment of a geothermal rotor exhibiting degradation. A case study will be reviewed and discussed covering a single flow rotor which developed erosion damage (flash cavitation/wire drawing) to the crest of the last stage disc fir tree. The objective of the assessment in this instance was to determine the remaining safe operating life of the rotor to enable a planned repair strategy to be proposed and implemented.

## 1. INTRODUCTION

To be competitive geothermal power plants have to operate efficiently, minimize unplanned outages and maximizing availability. Knowledge of the asset, operating conditions and damage mechanism is paramount in achieving these goals and to help the operator generate a life management plan for the asset from cradle to grave. This paper will look at the steps involved to achieve these goals including:

- Knowledge of the materials used in the steam path.
- Analysis of steam chemistry.
- Knowledge of degradation mechanism and which are applicable for the area of concern.
- Dimensions of the rotor, blades and diaphragms.
- Generation of a virtual model of the rotor and blading.
- Analysis of model to determine critical areas.
- Generation of an inspection test plan.
- Undertaking a fitness for service analysis after an outage inspection as required.

## 2. MATERIALS AND DESIGN USED IN STEAM PATH

The original equipment manufacturer (OEM) will have undertaken extensive testing and analysis of the design to ensure materials and design achieve the desired power generation and predicted life. Most of the testing and analysis will be proprietary and hence to enable the operator independence from the OEM will require independent analysis.

The operating manual for the geothermal rotor will contain details on the rotor material, blades and diaphragms. These do need to be checked especially on older units which may have experienced reworking or re-blading during the life of the unit. The development of portable x-ray fluorescent (XRF) analyzers enables this checking to be achieved during a scheduled outage. The analysis needs only to be completed once and only repeated when new/repaired components are installed into the steam path.

The common materials are:

- Rotor forgings — CrMoV, NiCrMoV, 410
- Blades, Coverbands and Diaphragms — 410/403, 15-3PH, 17-4PH, Ti6Al4
- Tie wires — 410/403
- Dovetail pins — CrMo low alloy steels
- Erosion Shields — Stellite Type 6B

For each material used in the steam path reference to NACE MR0175/ISO 15156 [1] should be undertaken to ensure the material is supplied in the best heat treatment condition for the service environment to minimize the likelihood of sulfide stress cracking (SSC).

The operation of the rotors requires a low stress design for a relatively low steam temperature (up to 280°C) so most of the rotors originate from the nuclear industry. The rotor forgings are now of the solid rotor type with integral discs with either a single or double flow configuration. Blade fixings are typically T roots (single or double), Straddle root fixings (radial fir tree) , axial fir tree and multi finger pinned root [2]. The design of the blading and rotor fir tree (hooks) is that on reaching full rotation speed the blade fixings are all engaged, and the load shared between each of the blade/rotor interface areas. This should be achieved within the elastic region of the stress strain curve for the blade and rotor to ensure no plastic deformation occurs. The interaction and fit of the blades on the rotor are critical when re-blading is required, and great care is needed to ensure load shedding across the blade/rotor interfaces occurs.

## 3. STEAM CHEMISTRY

The operating conditions in the geothermal steam path are the most hostile in the power generation process. The steam is not like conventional thermal steam plants with the process water and make up water treated and controlled to minimize corrosion and degradation in the plant. Geothermal steam typically has a small carryover from the steam separator or from dry steam wells. This can include heavy metals (such as mercury), acids (in gas phase or liquid) as well as silicon and chloride (sodium and calcium) the pH of the steam condensate can also vary significantly depending on the level of acid gas presents (HCl or Boric acid) present . The steam/brine from the geothermal well can change over the life of the geothermal resource and the monitoring of the steam quality, gas content and condensate chemistry is critical. Maintaining the axillary plant in the steam line, such scrubbers and separators, is critical in protecting the steam path parts from early degradation as well as the steam pipework. Examples of various geothermal resources are reported in [2, 3] and shown in Table 1.

**Table 1: Variation in steam purity as measured in condesates at five geothermal resources [2, 5]**

| Location | | Geyser U.S.A | | Matsukawa Japan | | Kakkonda Japan | | Cerro Prieto Mexico | | TIWI Philippines | |
|---|---|---|---|---|---|---|---|---|---|---|---|
| Steam Quality % | $H_2O$ | 98.05-99.51 | | 99.40-99.80 | | 99.85-99.97 | | 99.08-99.78 | | 98.43-99.16 | |
| | Gas | 0.49-1.95 | | 0.20-0.60 | | 0.03-0.15 | | 0.22-0.92 | | 0.83-1.67 | |
| Gases Content Vol% | $H_2S$ | 1.69-2.99 | | 12.9-17.7 | | 9-26 | | 20.9 | | 0.8-2.57 | |
| | $CO_2$ | 63.5-69.3 | | 79.3-85.2 | | 65-87 | | 79.1 | | 96.64-98.63 | |
| | Bal | 37.69-34.89 | | 1.7-4.2 | | 0.5-15 | | - | | 0.37-4.4 | |
| | | Condensate | Hot Water | Condensate | Hot Water | Condensate | Hot Water | Condensate | Hot Water | Condensate | Hot Water |
| Condensate and hot water (ppm) | pH | 6.5 | 6.7-7.3 | 4.4-4.9 | 4.4-5.3 | 6.0-6.4 | 8.8-9.1 | | 5.8-6.6 | 4.2-5.9 | 7.5 |
| | K | - | - | 0.3-3.0 | 120-300 | 0.1-0.28 | 55-67 | | 631-2031 | 0.07-0.37 | 830 |
| | Na | - | - | 0.8-5.0 | 152-360 | 0.27-0.72 | 460-501 | | 4406-7764 | 0.05-3.0 | 4400 |
| | Mg | <1 | - | <2.1 | 4.7-14.5 | <0.1 | 0.01-0.02 | - | - | 0.02-0.20 | 0.19 |
| | Ca | <1 | - | <1.6 | 12.8-28.8 | Trace | 5.8-9.0 | - | 259-359 | 0.02-0.20 | 85.0 |
| | Fe | <0.1 | - | 0.45-17.8 | 235-630 | 0.01-0.05 | 0.06-0.09 | - | - | <0.31 | 0.31 |
| | Al | - | - | <2.0 | 6.5-28.6 | 0.01-0.04 | 0.14-0.64 | - | - | Tr-0.20 | 0.14 |
| | Si | 0.71 | - | 0.83-4.7 | 273-566 | 0.22-0.52 | 256-364 | - | 179-1458 | 0.02-1.72 | 345 |
| | Cl | 39 | - | 3.3-6.7 | 4.3-13.8 | 1.9-3.4 | 625-685 | - | 928-14934 | 0.91-173 | 8970 |
| | $SO_4$ | 229 | - | 2.0-40 | 1188-1856 | 0.24-0.83 | 64-82 | - | 4.9-62 | 13.2-53.7 | 46.5 |
| | $CO_2$ | - | - | 12.4-51 | 4.3-6.5 | 14.40 | Trace | - | 42-494 | 106-108 | - |
| | $H_2S$ | 5-10 | 30-205 | 10-52.2 | 1.7-3.3 | 25-58 | 2.1-3.4 | - | 24-165 | 6.0-8.9 | - |

## 4. DEGRADATION MECHANISMS

The common degradation mechanisms encountered in the steam path parts are:

- Sulfide stress cracking (SSC).
- Moisture induced damage-impact erosion, flash cavitation/wire drawing, impact.
- Foreign object damage/ domestic object damage.
- Solid particle erosion, scale formation.
- Rubbing/abrasion.

These have been discussed and covered elsewhere [4] and reference to this document should be made for details of each type of damage mechanism listed. This paper covers the degradation generated by moisture induced damage.

Moisture induced damage in the geothermal steam path can generate extensive material degradation, reducing efficiency, lead to a reduction in operational period with forced outages occurring and ultimately the need for replacement of components. Within the Moisture induced damage classification there are four main forms of degradation:

- Moisture -impact erosion. This manifest itself mainly on the leading edge (suction side) of rotating blades near the outer diameter of the blades. The damage is generated by impact of water droplets on the surface of the blade and is similar to cavitation attack, see Figure 1 A.
- Trailing edge erosion. During low load operation the dual phase flow (steam and water) can recirculate onto the trailing edge of the last stage blade from the exhaust casing. The damage is found just above the platform on the suction face of the last stage blade, see Figure 1 B.
- Water washing erosion. This form of damage is generated when water flows over the material surfaces at high velocities It can be seen on the disc blade fixings while the 12 Cr martensite steel blades stand proud as these are slightly more resistant to the mechanism, see Figure 1 C.

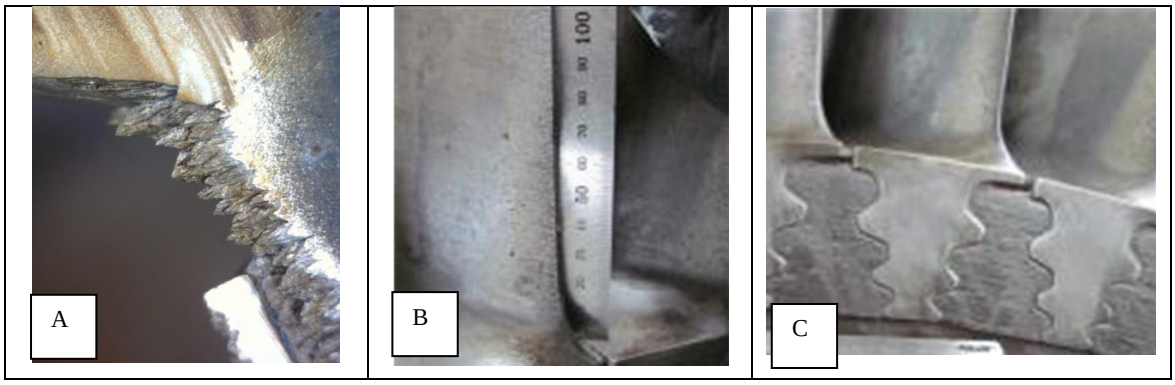


**Figure 1. A -Water Droplet Erosion on leading edge of blade. B-Trailing edge erosion. C- Water washing of disc steeples**

- Flash cavitation/wire drawing erosion. In the later stages of the turbine where two phases (steam and condensate liquid) exist, the condensate liquid phase can cause erosion damage when the liquid is forced by pressure differential to flow between surfaces and then flashes at lower pressure. Three conditions must exist for throttling/wire drawing erosion to occur
    - A two phase mixture must be present with a high pressure at the entrance to the leakage path.
    - A pressure differential across the surfaces/joint.
    - Presence of a primary leakage path through which the two phase fluid can pass and expand from high to lower pressure.

Progressing through the steam path these three requirements can be commonly found. Once the steam in a condensing unit has passed the saturation line, see Figure 2, the first two requirements will be present. The likelihood of the third requirement being present increases as a unit ages as leakage paths develop over time. This can be seen in the latter stages of the turbine notable between the crest of the disc blade fixings and the underside of the blade platforms. As the fluid expands through the small opening the water phase will cause deterioration and loss of material by flash cavitation/wire drawing effects opening up the aperture size and increasing the leakage quantity. It is this mechanism that causes the degradation in the rotor that will be assessed in this paper.

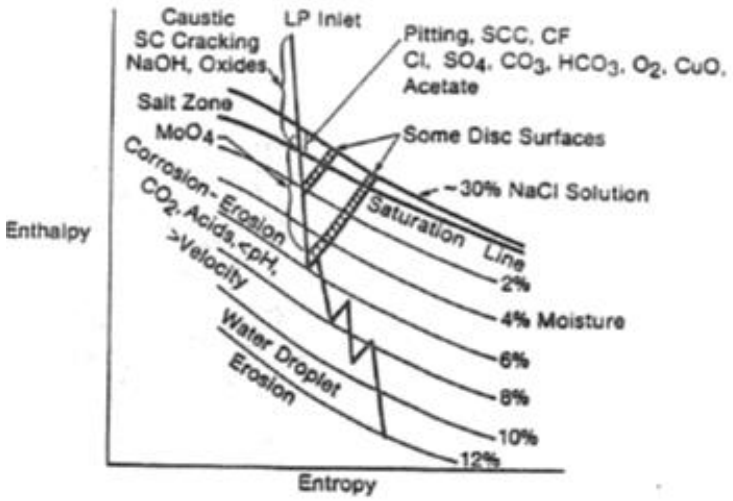


**Figure 2. Mollier Diagram showing typical expansion line through steam turbine and associated damage mechanisms as function of expansion of steam. [4]**

## 5. REMNANT LIFE ASSESSMENT AND FITNESS FOR SERVICE

To enable an independent analysis of the component the design, current condition and operational history need to be reviewed. The typical work flow for the assessment is shown in Figure 3

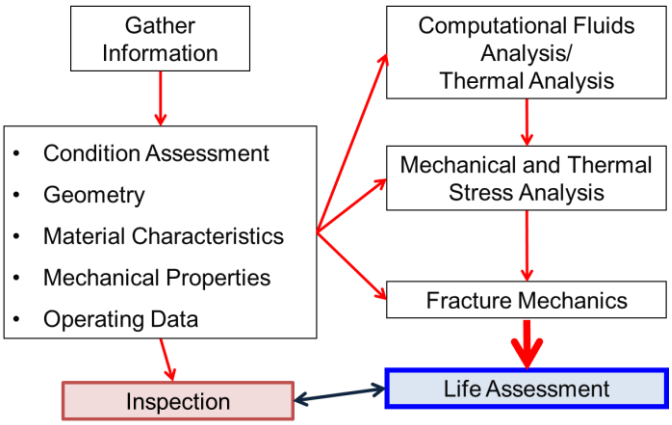


**Figure 3. Life assessment work flow.**

Ideally this process should be completed early in the life of the steam path components to enable a life management plan to be generated, however the process can be completed at any time during the life of the component. As Figure 3 illustrates assessment of the current condition, geometry and materials are assessed during a on-site inspection of the steam path parts. During the site inspection the following tasks should be competed:

- Collection of operational data, including maintenance, repairs and major incidents.
- Steam chemistry data for the operation of the unit.
- Condition assessment- visual inspection, metallurgical evaluation, mechanical testing (hardness), chemical analysis, non-destructive examination (UTPA, MPI, DPI and EC) and geometry of rotor, blades and diaphragms.

With the above data collected a generic model of the rotor can be generated. The analysis would identify the high risk/principal stress areas on the rotor requiring regular inspection. After the life assessment model is developed, in service issues detected during planned outages such as erosion and corrosion wastage can be rapidly assessed.

Typical appearance of a rotor after lifting of the top casing is shown in Figure 4. Condition assessment of this single flow rotor found material wastage on the crest of the disc fir tree of the last stage blade through an erosion/corrosion damage mechanism of the flash cavitation /wire drawing type, see Figure 5.

,

**Figure 4. Typical appearance of a single flow turbine after lifting top casing**

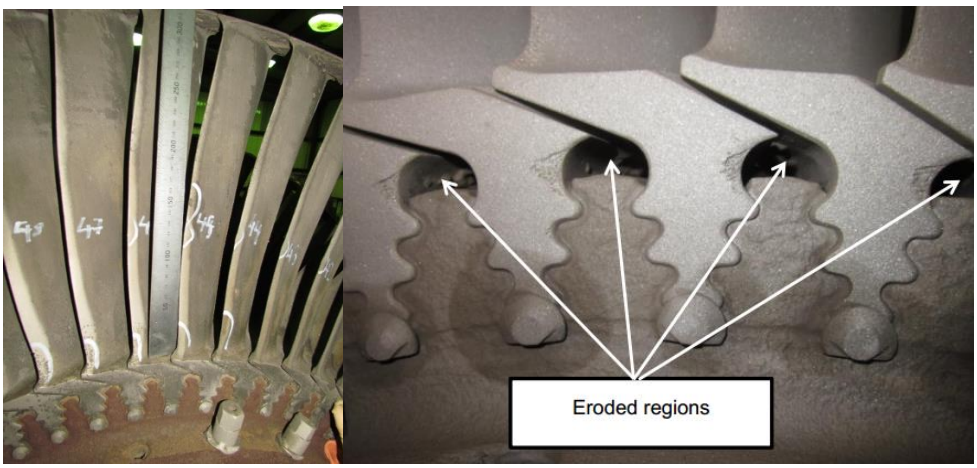


**Figure 5. Appearance of rotor before (left) and after cleaning (right) showing material loss from top of disc blade fixing crest due to flash cavitation/wire drawing erosion.**

Concerned that the loss of material from the top hook would compromise the blade fixing a fitness-for-service (FFS) was completed prior to returning the unit to service. The objectives of the FFS were to:

- Determine the mechanical stresses acting at the serrations of the stage 6 fir-tree root fixings in the corroded/eroded condition, for normal operation and over-speed conditions.
- Determine the fitness-for-service of the stage 6 disc by considering the margin between the calculated stresses and the yield strength.
- Determine critical crack size for the top serration where material erosion/corrosion had occurred in accordance with BS 7910 [5].
- Identify the safe operating window to enable a replacement rotor to be sourced and delivered whilst maintaining power generation.

The finite element analysis was undertaken using the symmetry of the rotor. There were 60 blades on the last stage disc and therefore a 6° sector of the final stage disc post and rotor was modelled, with symmetry boundary conditions on the symmetry faces as shown in Figure 6. Centrifugal loading was considered as the primary source of load in this instance. This was prescribed by defining the rotational speed of the rotor which was assumed conservatively to be a 10 per cent over speed, (i.e. 110 per cent of normal operational speed). Normal operation was at 60 Hertz or 377 radians per second, therefore a 10 per cent over speed of 414.7 radians per second was considered in the analysis. The centrifugal load was calculated on the entire finite element model using the prescribed material densities. However, since only the blade root was modelled, the mass of the aerofoil section of the turbine blade and the integral shroud was not included in this calculation these needed to be determine and added to centrifugal load. The calculation was based on calculating the cross-sectional area of the turbine blade at four separate heights of the blade. Denoting the area of each section by Ai, at a distance of Ri from the axis of revolution, the centrifugal load (F) was calculated as follows

$$F = \frac{1}{2}\rho\omega^2 \sum_{i+1}^{4} Ai\,(R_{i+1}^2 - R_i^2).$$

Here $\rho$ is the material density, ω is the rotational speed and $R_i$ is taken as the distance from the underside of the integral shroud to the axis of rotation. The results of these calculations are summarized in Table 2. The material density was taken to be 7750 kg/m3. The centrifugal load associated with the integral shroud was calculated separately and is summarized in Table 3.

**Table 2. Calculation of centrifugal load of un-modelled turbine blade mass**

| **Level** | $\boldsymbol{A_i}$**, (m)** | $\boldsymbol{R_i}$**,(m)** | $\boldsymbol{F_i = \frac{1}{2}\rho\omega^2 \sum_{i+1}^{4} Ai\,(R_{i+1}^2 - R_i^2).}$ |
|---|---|---|---|
| 1 | 0.00188029 | 0.4015 | 62,571.25 N |
| 2 | 0.00142855 | 0.4595 | 97,003.74 N |
| 3 | 0.00081812 | 0.5595 | 66,456.82 N |
| 4 | 0.00044302 | 0.6595 | 24,426.3 N |
| 5 (underside of shroud | | 0.7195 | |
| | | $F = \sum_{i=1}^{4} F_i$ | 250,459 N |

**Table 3. Calculation of centrifugal load of un-modelled shroud.**

| Quantity | Value | Unit | Notes |
|---|---|---|---|
| Integral shroud thickness (t) | 7.5 | mm | |
| Integral shroud with (w) | 45.174 | mm | |
| Integral shroud distance from axis of revolution (r) | 727 | mm | |
| Volume (V) (all Shrouds) | 1547619 | mm | $V=2\pi r.w.t$ |
| Density (ρ) | $7.75 \times 10^{-9}$ | $tonnes/mm^3$ | |
| Mass (m) | $1.24 \times 10^{-2}$ | tonnes | $m=\rho V$ |
| Rotation speed (ω) | 414.6902 | $Rad.s^{-1}$ | 10% overspeed |
| Number of blades (n) | 60 | | |
| Centrifugal load per shroud (F) | 24,992 | N | $F=m\omega^2 r/n$ |

Therefore, the total centrifugal load applied to the blade root area (to account for un-modelled blade and cover-band mass) is 250,459 N + 24,992 N = 275,451 N. This calculated centrifugal load was then used in the finite element model as a radial force distributed across the upper surface of the truncated geometry of the blade.

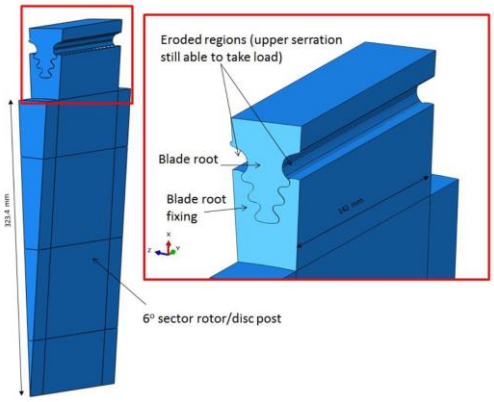


**Figure 6. Model geometry – 6° symmetry sector of final stage disc/rotor with blade root in fixing.**

From the geometry model the disc in question was isolated and the degradation to the top crest input into the model. The objective being to determine how the stress state in the disc changes due to increasing presence of erosion/corrosion to the crest of the disc steeple and at what point the blade would be released. The model was meshed with a swept/structured mesh with second order hexahedral elements (20 nodes), with refinement at the areas of anticipated high stress (roots of the disc steeple hooks), see Figure 7. The analysis ranged from the current condition with remnants of the top hook to when the top hook was removed completly and all the loads were applied to the bottom two hooks.

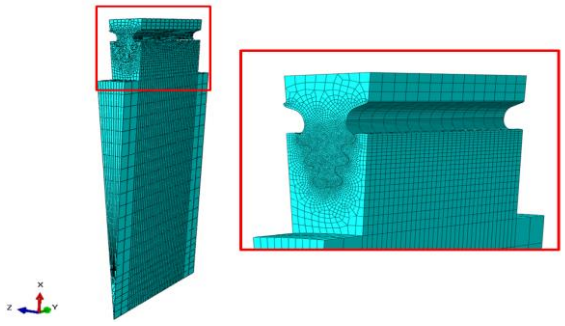

**Figure 7. Modelled geometry with erosion damage taken into account.**

Finite element analysis applying the blade loading to the disc fixing with the reduced section size of the top hook was completed. The disc material had been identified/confirmed during the condition assessment as a 3.5NiCrMoV steel and was assumed to have the following material properties, see Table 4

**Table 4. Material properties assumed for rotor disc.**

| **Disc Material Data** | |
|---|---|
| Young Modulus | 212 GPa |
| Poisson's Ratio | 0.3 |
| Density | $7.75x10^{-9}$ tonnes/$mm^3$ |
| Minimum Yield Strength | 650 MPa |
| Minimum UTS | 930 MPa |

The peak stress calculated by finite element analysis using the generated model that considered a conservative estimate of the current condition of the top hook erosion/corrosion was 563 MPa (von Mises) and occurred at the uppermost serration of the blade root fixing, see Figure 7 and Table 5. This high stress was primarily due to the loss of material at this location.

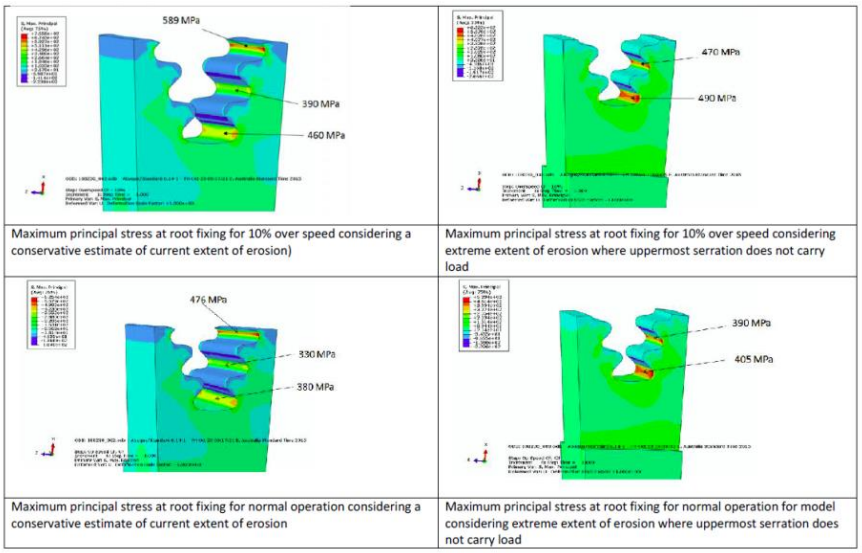


**Figure 8. Peak stress found at various erosion states of the top hook at 10 % overspeed and normal operation.**

**Table 5. Peak stress determined, and margin compared to yield stress**

| **Model** | **Peak maximum principal stress(MPa)** | **Peak von Mises stress (MPa)** | **Location/ serration** | **Margin on yield** |
|---|---|---|---|---|
| Conservative estimate of current state of erosion | 589 | 563 | uppermost | **13 %** |
| | 390 | 346 | middle | 46 % |
| | 460 | 414 | lowermost | 36 % |
| Extreme state of erosion (upper most serrations eroded away) | 470 | 417 | middle | 35 % |
| | 490 | 432 | lowermost | 33 % |

Given the material properties shown in Table 4 for the rotor material 3.5NiCrMoV and comparing the peak stress indicated by the analysis it is considered that the disc could be operated at normal operating conditions in its current condition even when the top hook was completely lost.

Based on the finite element analysis results a critical flaw size calculation was performed at the highest stressed radius in the root fixing. The results of this critical flaw size calculation provide an indication of the tolerance to flaws that may be found in future inspection or for cracks that are below the detectable inspection limit. If flaws are found in the future at the locations considered in this assessment it is advised that further analysis be undertaken which would include a fatigue crack growth assessment of the flaws to determine the safe life before they reach a critical size which could result in failure.

For this assessment a fracture toughness of 180 $MPam^{-1/2}$ was used and was sourced from [9].

The critical flaw size was calculated using Signal FFS™ (commercially available software developed by Quest Integrity), with the critical flaw size calculations determined as per BS 7910 [8]. The critical flaw size was calculated based on flat plate fracture mechanics idealisation. The dimensions of the flat plate idealisation were taken from key dimensions relating to the blade root fixing as presented in Table 6.

**Table 6. Dimensions of fracture mechanics idealisations**

| Model | Location | Plate width (mm) | Plate length (mm) |
|---|---|---|---|
| Conservative estimate of current state of erosion | Uppermost serration | 142 | 3.8 |
| Extreme state of erosion (upper most serrations eroded away) | Lowermost serration | 142 | 7.2 |

An illustration of how the flat plate dimensions are derived is provided in Figure 9.

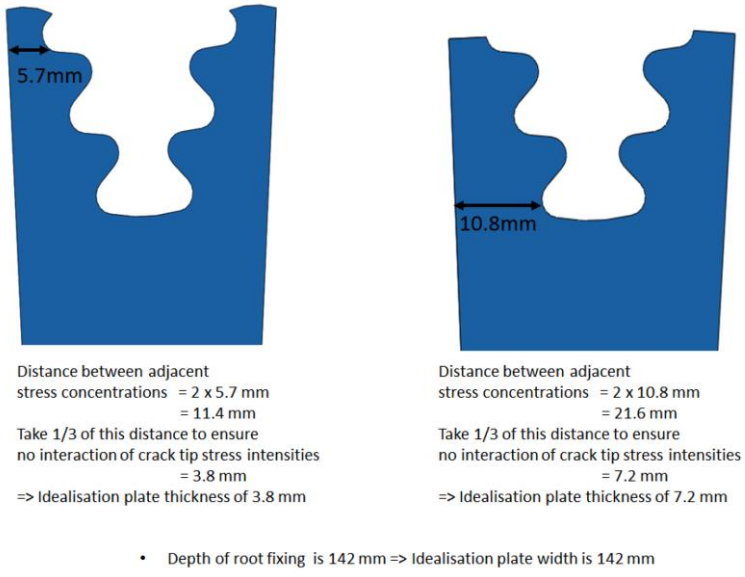


**Figure 9. Illustration of how dimensions of fracture mechanics idealisation are derived**

The stress profiles for the conservative estimate of the current state of erosion and the extreme state of erosion where the uppermost serrations have eroded away are shown in Figure 10 and Figure 11 respectively. It should be noted that only mechanical loading was considered for the fracture mechanics assessment. The assessment has not taken account of any thermal stresses that may be generated during a start.

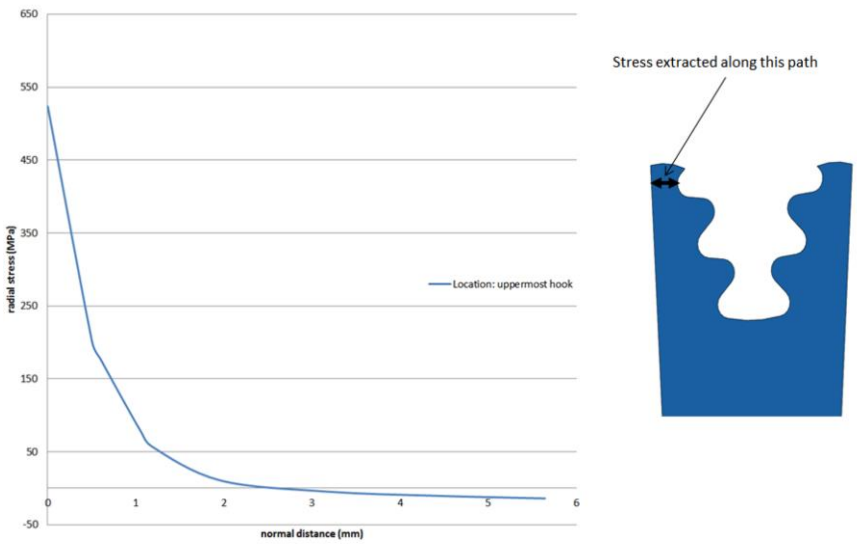


**Figure 10. Radial stress as a function of normal distance from peak stress concentration at uppermost fir tree hook for conservative estimate of current corrosion.**

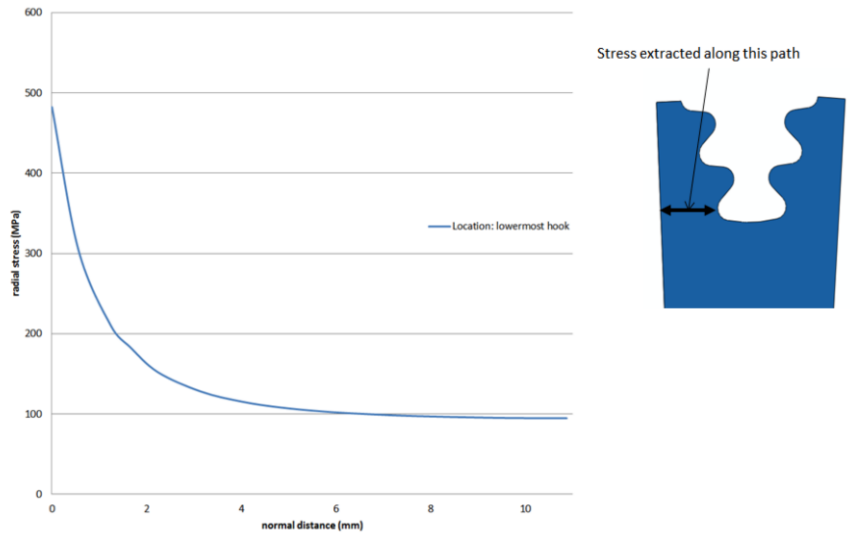


**Figure 11. Radial stress as a function of normal distance from peak stress concentration at lowermost serration for extreme extent of erosion where uppermost serration is no longer present**

The calculated critical flaw sizes for flaws extending the entire length of blade root fixing are shown in Table 7.

**Table 7. Critical flaw depths for flaws extending the entire length of blade root fixing (10 per cent over speed condition)**

| Model | Location | Flaw depth (mm) |
|---|---|---|
| Conservative estimate of current state of erosion | Uppermost serration | 2.7 |
| Extreme state of erosion (upper most serrations eroded away) | Lowermost serration | 4.1 |

By considering a 1 mm deep flaw extending the entire width of the blade root fixing, the associated assessment point for such a flaw could be plotted on a failure assessment diagram (FAD) as per BS 7910. The FAD provides a means of assessing pre-existing flaws

for their acceptability and margin against brittle fracture and ductile overload. This assessment point may then be compared to the assessment point for the critical flaw size in order to calculate the associated reserve load factor, which in turn provides a measure of the margin on load associated with a potential pre-existing (1 mm deep) flaw. This is a conservative means of assessing the margin on load for a potential defect that may have been missed during inspection.

The associated reserve load factor calculations for the conservative estimate of the current state of erosion and the extreme state of erosion, where the uppermost serrations have eroded away are shown in Figure 12 and Figure 13 respectively. The associated reserve load factors are summarised in Table 8.

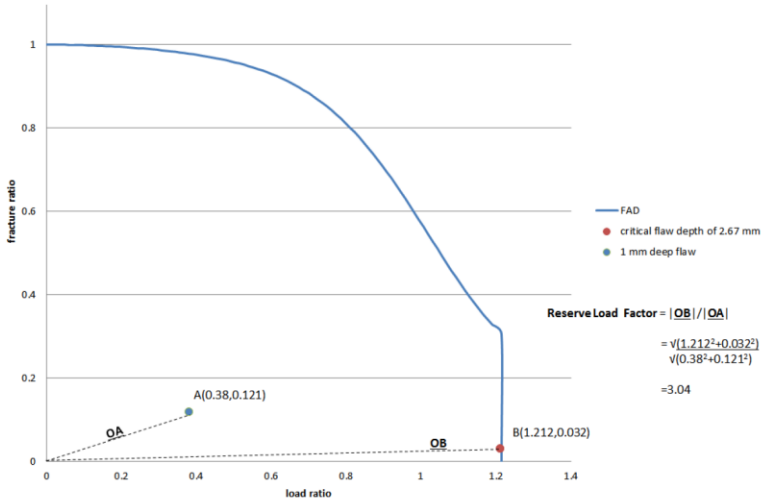


**Figure 12. Illustration of reserve load factor calculation for the conservative erosion at the current state of corrosion (critical location at uppermost serration)**

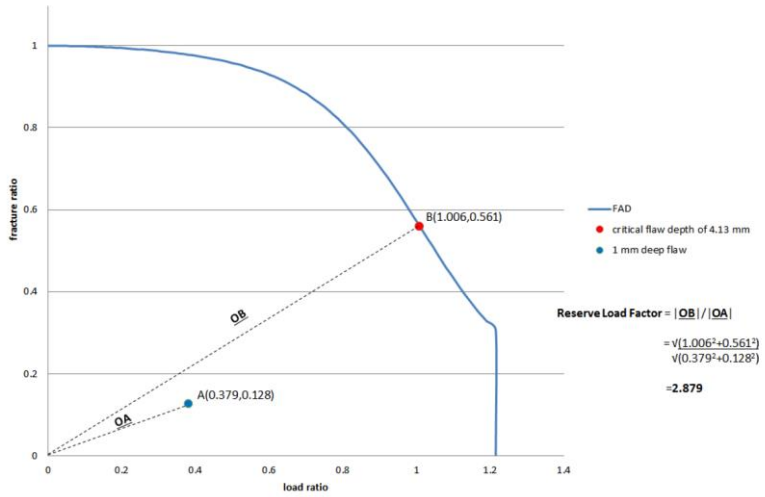


**Figure 13. Illustration of reserve load factor calculation for the extreme case erosion for when the uppermost serration is not present (critical location at lowermost serration)**

**Table 8. Reserve load factors associated with a 1 mm deep crack extending the entire length of the fir tree slot/root – based on 10 per cent over speed**

| Model | Location | Reserve load factor |
|---|---|---|
| Conservative estimate of current state of erosion | Uppermost serration | 3.04 |
| Extreme state of erosion (upper most serrations eroded away) | Lowermost serration | 2.88 |

It is of interest to note that for the conservative estimate of the current state of erosion where the critical location is at the uppermost serrations, the FAD indicates that the failure mode is almost entirely ductile overload. This is shown by the assessment point being to the far right on the FAD with a low fracture ratio. This is expected as the critical crack depth is 2.7 mm compared to the assumed

thickness of 3.8 mm, i.e. the remaining ligament is small and likely to suffer from ductile overload. For the extreme case of erosion where the upper serrations have been assumed to have eroded away and the critical location is at the lower most serration, the position of the assessment point on the FAD indicates failure from a combination of fracture initiation and ductile overload. This is to be expected due to the increased thickness of the lower serration compared to the upper serration.

It is seen from Table 8 that reserve load factors greater than unity are calculated for both the model that considers the current state of erosion and the model that considers the extreme state of erosion where the upper most serrations have eroded away, indicating sufficient margin on load in the context of the BS 7910 FAD.

Note: load is proportional to the square of rotational speed. Therefore, the reserve factor on speed is obtained by taking the square root of the reserve load factor (see Table 7). Note, these reserve load factors have been calculated based on 10 per cent over speed conditions. Therefore, reserve on operational speed of 3600 rpm is also shown in the last column of Table 9 (calculated by multiplying the reserve factor on 10 per cent over speed by a factor of 1.1).

**Table 9. Reserve factor on operational speed (based on 1 mm deep flaw**

| Model | Location | Reserve load factor | Reserve load factor on speed compared to 10% overspeed | Reserve factor on speed compared to normal operation (3600rpm) |
|---|---|---|---|---|
| Conservative estimate of current state of erosion | Uppermost serration | 3.04 | 1.74 | 1.92 |
| Extreme state of erosion (upper most serrations eroded away) | Lowermost serration | 2.88 | 1.70 | 1.87 |

Comparing the degradation recorded during the condition assessment inspections the rotor should achieve the operating life required to enable a replacement rotor to be sourced, manufactured and installed.

## 5. CONCLUSIONS

On completion of the rotor life management exercise it was possible to develop component inspection management programmes for the rotor that were based on a sound technical approach as outlined in technical publications based on fitness-for-service guidelines (i.e. BS7910 or API 579).

Knowing the current condition of the rotor and steam path parts and damage mechanisms, it is possible to specify future inspection frequencies for the rotor dependant on the current condition and the damage detected during the condition assessment and inspection.

Whenever degradation/damage is identified the data in a life management plan can enable fitness for service analysis to be completed rapidly to ensure engineering operation decisions are made minimising risk and maintaining the availability of the generating capacity until a scheduled outage can be planned. The example discussed here shows that a planned repair/replacement could be scheduled instead of a forced and extended outage with immediate and possibly long-term loss of generation.

## REFERENCES

[1]. International Standard ANSI/NACE MR0175/ISO 15156-1/2/3 Petroleum and Natural Gas Industries – Materials for Use in H2S Containing Environments in Oil and Gas Production, NACE International (2009).

[2] Sander W.P.: Turbine Steam Path Maintenance and Repair volume 1, Pennwell Corporation .

[3]. DiPippo R: Geothermal Power Plants, Elsevier 2012

[4]. Rowbotham, S.P , Chung, O, Ko, M and Wong, J. : Failure Mechanisms Encountered in Geothermal Steam Service.

[5]. BS 7910:2013, Guide to methods for assessing the acceptability of flaws in metallic structures, British Standard Institution.

[6].McNaughton, W.P., Richman, R.H. and Jaffee, R.I., 1991. ““Superclean” 3.5NiCrMoV Turbine Rotor Steel: A Status Report – Part II: Mechanical Properties”, Journal of Materials Engineering, Volume 13 Number 1 pg 19 -28.